Am J Transl Res 2025;17(9):7058-7066
www.ajtr.org /ISSN:1943-8141/AJTR0166093

Original Article

Development and validation of a nomogram for predicting moderate-to-severe pain in hepatitis B virus-related liver cancer patients after CyberKnife treatment

Yating Chi[1*], Jing Yang[1*], Guona Li[2], Jun Jia[3]

[1]Jingzhong Medical Zone, Chinese PLA General Hospital, Beijing, China; [2]Department of Hematology, The Fifth Medical Center of Chinese PLA General Hospital, Beijing, China; [3]Department of Radiotherapy, Senior Department of Oncology, Chinese PLA General Hospital, Beijing, China. [*]Equal contributors and co-first authors.

Received May 16, 2025; Accepted August 11, 2025; Epub September 15, 2025; Published September 30, 2025

Abstract: Objective: To identify risk factors for moderate-to-severe pain after CyberKnife treatment in patients with hepatitis B virus - related liver cancer and to develop a predictive nomogram. Methods: This retrospective study included 169 patients treated between April 2021 and August 2022 as the derivation cohort, and 132 patients treated between September 2022 and October 2024 as the validation cohort, all at the Fifth Medical Center of Chinese PLA General Hospital. Univariate and multivariate logistic regression analyses were conducted in the derivation cohort to identify independent predictors, which were then incorporated into a nomogram. Predictive performance was evaluated using receiver operating characteristic (ROC) curves in both cohorts. Results: Moderate-to-severe postoperative pain occurred in 57/169 patients (33.73%) in the derivation cohort and 45/132 (34.09%) in the validation cohort. Multivariate analysis identified four independent risk factors: tumor invasion of the liver capsule, Child-Pugh class B, cirrhosis, and tumor size ≥5 cm (all $P<0.05$). The nomogram achieved an AUC of 0.700 in the derivation cohort and 0.685 in the validation cohort, indicating acceptable discrimination. Conclusions: Tumor proximity to the liver capsule, impaired baseline liver function, cirrhosis, and large tumor size were significant predictors of moderate-to-severe postoperative pain after CyberKnife treatment. The developed nomogram demonstrated robust internal and external validity, offering a practical tool for preoperative risk stratification and individualized analgesic planning.

Keywords: Hepatitis B virus, liver cancer, CyberKnife, moderately severe pain, risk factors

Introduction

Hepatitis B virus (HBV) infection is a major risk factor for hepatocellular carcinoma (HCC), accounting for approximately 54% of global HCC cases [1]. Precision radiotherapy, particularly CyberKnife, has become a critical option for inoperable or surgically intolerant HCC patients due to its high accuracy, noninvasiveness, and minimal damage to surrounding tissues [2, 3]. Despite its advantages in local tumor control, CyberKnife therapy can cause adverse effects, with moderate-to-severe pain being a notable clinical challenge [4]. Such pain may result from radiation-induced liver injury, tumor necrosis, or inflammatory responses in adjacent organs [5, 6].

Most previous studies have addressed pain symptoms and empirical treatments (e.g., opioids) without systematically exploring risk factors in the HBV-related HCC population [7, 8]. Although thrombocytopenia and impaired liver function have been tentatively linked to pain intensity, these investigations often overlook HBV-specific features, such as the high prevalence of liver fibrosis/cirrhosis and exposure to antiviral therapy [9, 10]. Furthermore, studies rarely distinguish between HCC etiologies (HBV vs. HCV or alcohol-related), despite distinct tumor microenvironments and treatment responses [11, 12].

Chronic HBV infection often progresses to cirrhosis, altering the hepatic microenvironment

https://doi.org/10.62347/HRDH6927

through sinusoidal capillarization and capsular fibrosis, which may increase mechanical sensitivity and hinder tissue repair after radiotherapy [13]. Inadequate antiviral therapy, with persistent viral replication, could exacerbate radiation-induced inflammation, yet this interaction remains poorly studied [14]. Existing risk assessment tools seldom incorporate HBV-specific findings (e.g., Child-Pugh status, cirrhosis history) [15].

This study aims to identify independent risk factors for moderate-to-severe pain in HBV-related HCC patients after CyberKnife treatment, develop and validate a nomogram for individualized pain risk prediction. This should provide a tailored framework for optimizing postoperative analgesic strategy in this high-prevalence subgroup.

Materials and methods

This retrospective study included 169 patients with HBV - related HCC who underwent CyberKnife treatment at the Fifth Medical Center of Chinese PLA General Hospital between April 2021 and August 2022 as the modeling cohort. An additional 132 patients treated between September 2022 and October 2024 served as the validation cohort. The study was approved by the Ethics Committee of the Fifth Medical Center of Chinese PLA General Hospital. All procedures involving human participants were conducted in accordance with the Declaration of Helsinki (as revised in 2013).

Inclusion criteria

Radiologic (contrast-enhanced CT/MRI) or histopathologic confirmation of HCC [16]; evidence of HBV infection (HBsAg positivity or serum HBV DNA ≥20 IU/mL); completion of standardized CyberKnife stereotactic body radiotherapy (prescription dose: 30-50 Gy in 3-5 fractions, target coverage ≥95%); age ≥18 years; Eastern Cooperative Oncology Group (ECOG) performance status ≤2; available data on liver function (Child-Pugh classification), tumor characteristics (diameter, proximity to liver capsule ≤1 cm, vascular invasion), cirrhosis status (imaging or histopathologic confirmation), HBV virological markers (DNA load, history of antiviral therapy), and comorbidities (hypertension, diabetes).

Exclusion criteria

Patients with other malignancies or pain from causes unrelated to liver cancer (e.g., abdominal infection, bone metastases); those with pre-existing moderate-to-severe pain or a history of long-term opioid use; patients receiving combined local therapies (e.g., radiofrequency ablation) or systemic chemotherapy alongside radiotherapy; patients with mental illness or inability to complete pain assessments; and those with severe cirrhosis-related complications (e.g., Child-Pugh class C, hepatic encephalopathy) that could confound postoperative pain evaluation.

Pain assessment

One week after treatment, pain was assessed using the Numerical Rating Scale (NRS), a validated patient-reported tool for quantifying pain intensity [7]. Scores range from 0 (no pain) to 10 (worst imaginable pain), with higher scores indicating greater intensity. Patients with NRS ≥4 were classified as having moderate-to-severe pain. In such cases, intramuscular tramadol or morphine was administered for analgesia.

Data collection

Data on possible factors associated with moderate-to-severe pain were collected before and after treatment, including sex, age, educational level, hypertension, diabetes, HBV status, cirrhosis [17], HBV DNA quantification [18], Child-Pugh classification [19], tumor size, tumor invasion of the liver capsule (≤1 cm) [20], tumor location, number of tumors, and vascular invasion [14].

Statistical analysis

Analyses were performed using SPSS version 29.0 (SPSS Inc., Chicago, IL, USA). Non-normally distributed continuous variables were analyzed using the Kruskal-Wallis or Mann-Whitney U tests. Categorical variables, expressed as counts and percentage, were compared using the chi-square test. Nomogram construction was performed in Python (version 3.13) using the scikit-learn (version 1.0.2) and matplotlib (version 3.5.1) libraries. Independent risk factors identified by multivariate logistic regression (tumor invasion of the liver capsule, Child-

Pugh class B, cirrhosis, and tumor size ≥5 cm) were assigned scores based on regression coefficients. The total score, obtained by summing individual factor scores, was mapped to the "Risk" axis to estimate the probability of moderate-to-severe postoperative pain. ROC curves were generated using predicted probabilities from the nomogram and actual pain outcomes (0 = no, 1 = yes). The area under the curve (AUC) was calculated to assess predictive performance. Graphs, including the nomogram and ROC curve, were generated using built-in statistical software functions. A *P*-value <0.05 was considered significant. Unless otherwise specified, values are expressed as mean ± standard deviation.

Results

Comparison of clinical data

Baseline characteristics did not differ significantly between the cohorts. Variables including age, sex, educational level, hypertension, diabetes, HBV DNA quantification, cirrhosis, Child-Pugh classification, tumor size, tumor invasion of the liver capsule, and other clinical findings were comparable (all P>0.05), indicating balanced baseline profiles (**Table 1**).

In the derivation cohort, 57 of 169 patients experienced moderate-to-severe postoperative pain, yielding an incidence of 33.73%. In the validation cohort, 45 of 132 patients (34.09%) reported moderate-to-severe pain.

Univariate analysis in the derivation cohort

Univariate analysis identified five factors significantly associated with moderate-to-severe postoperative pain (all P<0.05; **Table 2**): Cirrhosis of the liver (OR = 1.847, 95% CI: 1.203-2.837, P = 0.009); Child-Pugh class B (OR = 1.623, 95% CI: 1.152-2.286, P = 0.006); Tumor size ≥5 cm (OR = 2.113, 95% CI: 1.305-3.142, P = 0.005); Tumor invasion of liver capsule (OR = 1.610, 95% CI: 1.017-2.418, P = 0.030); Vascular invasion (OR = 2.514, 95% CI: 1.503-4.152, P<0.001).

No significant associations were found for age, BMI, serum albumin, total bilirubin, AFP, CyberKnife dose, educational level, hypertension, diabetes, HBV DNA quantification, tumor location, tumor number, smoking, alcohol use, BCLC stage, portal vein tumor thrombus, targeted therapy use, or opioid usage rate (all P>0.05).

Multivariate logistic regression in the derivation cohort

Variables significant in the univariate analysis were entered into a multivariate logistic regression model (coding shown in **Table 3**). Four factors remained independently associated with moderate-to-severe postoperative pain (all P<0.05; **Table 4**): Tumor invasion of liver capsule (OR = 3.853, 95% CI: 2.107-7.048, P<0.001); Child-Pugh class B (OR = 2.953, 95% CI: 1.652-5.283, P = 0.001); Cirrhosis of the liver (OR = 2.483, 95% CI: 1.352-4.562, P = 0.004); Tumor size ≥5 cm (OR = 2.623, 95% CI: 1.482-4.643, P = 0.002).

Nomogram construction

A nomogram was developed based on these four independent predictors (**Figure 1**). The prediction formula was: Linear Predictor (LP) = $1.769 \times X_1 + 1.703 \times X_2 + 1.622 \times X_3 + 1.576 \times X_4$. Where X_1 = tumor invasion of the liver capsule (0 = No, 1 = Yes), X_2 = Child-Pugh class (0 = A, 1 = B), X_3 = cirrhosis (0 = No, 1 = Yes), X_4 = tumor size (0 = <5 cm, 1 = ≥5 cm).

The probability of moderate-to-severe pain was calculated as $P = 1/[1 + \exp(-LP)]$.

Each variable was assigned a point value proportional to its regression coefficient. The sum of these points was mapped to the "Risk" axis to provide an individualized pain probability, supporting tailored analgesic planning.

ROC curve analysis

ROC curve analysis in the derivation cohort yielded an AUC of 0.700, indicating acceptable discrimination for predicting moderate-to-severe postoperative pain (**Figure 2**).

Discussion

HBV-related HCC remains a significant global health challenge, with oncogenesis strongly linked to chronic HBV infection [21, 22]. CyberKnife stereotactic body radiotherapy, noted for its submillimeter precision and real-time image guidance, is an established treatment for unresectable HCC [23, 24]. However, as its

Table 1. Comparison of clinical data

Variable	Modeling group (n = 169)	Validation group (n = 132)	χ^2/t	P
Age (years)	57.8±17.37	60.14±16.56	-1.185	0.237
Age				
≥60 years	96 (56.80)	85 (64.39)	5.006	0.025
<60 years	73 (43.20)	46 (35.61)		
Gender				
Male	106 (62.72)	116 (61.36)	0.002	0.963
Female	63 (37.28)	16 (38.64)		
Level of education				
High school and below	44 (26.04%)	46 (34.85%)	2.342	0.126
College and above	125 (73.96%)	86 (65.15%)		
Hypertension				
Yes	133 (78.7%)	93 (70.45%)	2.27	0.132
No	36 (21.3%)	39 (29.55%)		
Diabetes				
Yes	149 (88.17%)	113 (85.61%)	0.233	0.629
No	20 (11.83%)	19 (14.39%)		
Hepatitis B virus quantitative				
<1000 copies/ml	82 (48.52%)	50 (37.88%)	2.99	0.084
≥1000 copies/ml	87 (51.48%)	82 (62.12%)		
Cirrhosis of the liver				
Yes	86 (50.89%)	57 (43.18%)	1.469	0.225
No	83 (49.11%)	75 (56.82%)		
Child-Pugh classification				
A	77 (45.56%)	55 (41.67%)	0.312	0.576
B	92 (54.44%)	77 (58.33%)		
Tumor size				
≥5 cm	103 (60.95%)	73 (55.3%)	0.754	0.385
<5 cm	66 (39.05%)	59 (44.7%)		
Tumor invasion of liver capsule				
Yes	95 (56.21%)	68 (51.52%)	0.483	0.487
No	74 (43.79%)	64 (48.48%)		
Tumor location				
Peripheral type	104 (61.54%)	71 (53.79%)	1.525	0.217
Central type	65 (38.46%)	61 (46.21%)		
Number of tumors				
Individual	62 (36.69%)	53 (40.15%)	0.244	0.621
Multiple	107 (63.31%)	79 (59.85%)		
Vascular invasion				
Yes	87 (51.48%)	54 (40.91%)	2.915	0.088
No	82 (48.52%)	78 (59.09%)		
Smoking history (pack-years ≥10)				
Yes	107 (63.31%)	81 (61.36%)	0.051	0.821
No	62 (36.69%)	51 (38.64%)		
Alcohol consumption (g/day ≥30)				
Yes	113 (66.86%)	85 (64.39%)	0.106	0.745
No	56 (33.14%)	47 (35.61%)		
Body mass index (BMI, kg/m^2)	23.64±2.93	23.87±3.39	-0.625	0.532
Serum albumin (g/L)	40.02±5.63	39.78±5.2	0.376	0.707

Total bilirubin (μmol/L)	17.74±9.75	17.68±9.42	0.057	0.955
Alpha-Fetoprotein (AFP, log ng/mL)	2.45±1.05	2.58±1.05	-1.086	0.278
Maximum tumor size (cm)	4.97±2.4	5.23±2.33	-0.953	0.341
BCLC stage (B/C)			0.001	0.998
B	47 (27.81%)	37 (28.03%)		
C	122 (72.19%)	95 (71.97%)		
Portal vein tumor thrombus			0.011	0.916
Yes	144 (85.21%)	111 (84.09%)		
No	25 (14.79%)	21 (15.91%)		
CyberKnife dose (Gy)	50.8±4.24	50.11±4.23	1.399	0.163
Proportion of combined targeted therapy			2.958	0.085
Yes	149 (88.17%)	106 (80.3%)		
No	20 (11.83%)	26 (19.7%)		
Opioid usage rate			0.558	0.455
Opioid use	84 (49.7%)	59 (44.7%)		
No opioid use	85 (50.3%)	73 (55.3%)		
Moderate-to-severe pain rate			0.004	0.948
Moderate	112 (66.27%)	87 (65.91%)		
Severe	57 (33.73%)	45 (34.09%)		

Table 2. Univariate analysis results

Variable	OR (95% CI)	*P*-value
Age	0.989 (0.971-1.007)	0.227
BMI	0.934 (0.837-1.042)	0.221
Serum albumin	0.954 (0.900-1.011)	0.110
Total bilirubin	1.035 (0.997-1.075)	0.070
AFP	1.031 (0.744-1.429)	0.855
Max tumor size	0.972 (0.851-1.109)	0.671
CyberKnife dose	0.959 (0.890-1.035)	0.281
Level of education	0.565 (0.280-1.140)	0.111
Hypertension	0.885 (0.407-1.928)	0.759
Diabetes	0.754 (0.274-2.076)	0.585
Hepatitis B virus quantitative	0.541 (0.286-1.025)	0.060
Cirrhosis of the liver	1.847 (1.203-2.837)	0.009
Child-Pugh class B	1.623 (1.152-2.286)	0.006
Tumor size ≥5 cm	2.113 (1.305-3.142)	0.005
Tumor invasion of liver capsule	1.612 (1.017-2.418)	0.030
Tumor location	0.711 (0.368-1.374)	0.310
Number of tumors	0.645 (0.337-1.233)	0.185
Vascular invasion	2.514 (1.503-4.152)	<0.001
Smoking history (pack-years ≥10)	0.798 (0.412-1.545)	0.503
Alcohol consumption (g/day ≥30)	0.902 (0.460-1.768)	0.763
BCLC stage (B/C)	0.582 (0.292-1.159)	0.124
Portal vein tumor thrombus	0.668 (0.262-1.703)	0.398
Proportion of combined targeted therapy	0.754 (0.274-2.076)	0.585
Opioid usage rate	0.583 (0.308-1.103)	0.097

use expands, postoperative pain has emerged as a critical factor influencing treatment tolerability and patient quality of life. Radiation-induced liver injury - associated pain involves complex mechanisms, including hepatic capsule stretching, inflammatory mediator release (e.g., prostaglandin E2, bradykinin), and peripheral nerve sensitization [25, 26]. Although tumor location and baseline liver function have been implicated in pain risk, systematic risk factor analysis tailored to HBV-related HCC - characterized by distinct fibrosis - cirrhosis pathways and antiviral therapy contexts - remains limited [27, 28]. This gap hampers early identification and preventive analgesia, compromising adherence and long-term outcome.

Our multivariate analysis identified four independent predictors of moderate-to-severe postoperative pain: tumor invasion of the liver capsule, Child-Pugh class B, cirrhosis, and tumor size ≥5 cm. Capsule-adjacent tumors (≤1 cm) had the highest impact, likely due to radiation-induced capsular edema amplifying mechani-

Table 3. Multi-factor analysis assignment table

Factor	The assignment
Cirrhosis of the liver	No = 0; Yes = 1
Child-Pugh B	A = 0; B = 1
Tumor size	<5 cm = 0; ≥5 cm = 1
Tumor invasion of liver capsule	No = 0; Yes = 1
Vascular invasion	No = 0; Yes = 1

Table 4. Multivariate Logistic regression analysis

Factor	b	S.E	χ^2	P	OR	95% CI
Tumor invasion of liver capsule	1.348	0.308	19.110	<0.001	3.853	2.107-7.048
Child-Pugh class B	1.083	0.297	13.320	<0.001	2.953	1.652-5.283
Cirrhosis of the liver	0.910	0.311	8.580	0.003	2.483	1.352-4.562
Tumor size ≥5 cm	0.964	0.291	10.960	0.001	2.623	1.482-4.643

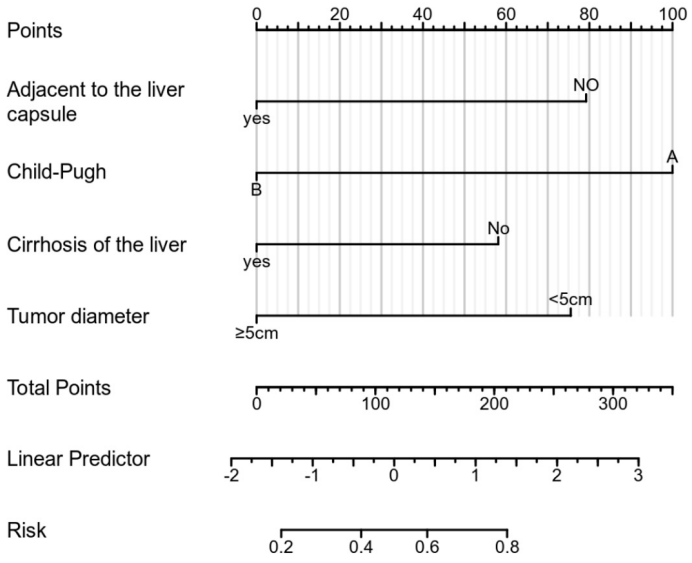

Figure 1. Nomogram model for predicting moderate to severe postoperative pain.

cal tension and nociceptor activation [29-31]. Child-Pugh class B patients had a 5.49-fold higher risk, possibly reflecting impaired clearance of pro-nociceptive mediators [13, 32, 33]. Cirrhosis increased risk through microcirculatory dysfunction and capsular fibrosis [14, 15, 34].

Larger tumors (≥5 cm) exhibited a clear "volume effect", in which higher radiation doses were required, leading to more extensive parenchymal injury and direct compression of peritumoral nerves [35-37]. The nomogram developed in this study maintained stable predictive performance in the validation cohort, likely due to rigorous case selection and highly standardized CyberKnife treatment parameters, ensuring robust discrimination across heterogeneous patient populations. Clinically, patients with multiple concurrent risk factors may benefit from a stepwise preventive analgesic strategy - such as combining selective COX-2 inhibitors with weak opioids - to address both peripheral inflammatory responses and central sensitization, consistent with the multimodal analgesia concept advocated by the International Association for the Study of Pain [38, 39].

Our findings align with existing literature. Tumor invasion of the liver capsule has been widely recognized as a strong pain trigger due to the capsule's rich innervation and susceptibility to mechanical stretch or inflammation from radiation-induced edema or tumor progression [40, 41]. Cirrhosis similarly increases susceptibility to pain through fibrotic remodeling and microcirculatory alterations that enhance tissue sensitivity to radiation injury [42, 43]. Impaired liver function, as reflected in higher Child-Pugh classification, may further contribute by reducing the clearance of pro-inflammatory mediators, thereby lowering pain thresholds [16, 44, 45]. Larger tumors not only demand higher radiation doses but also exert greater mechanical

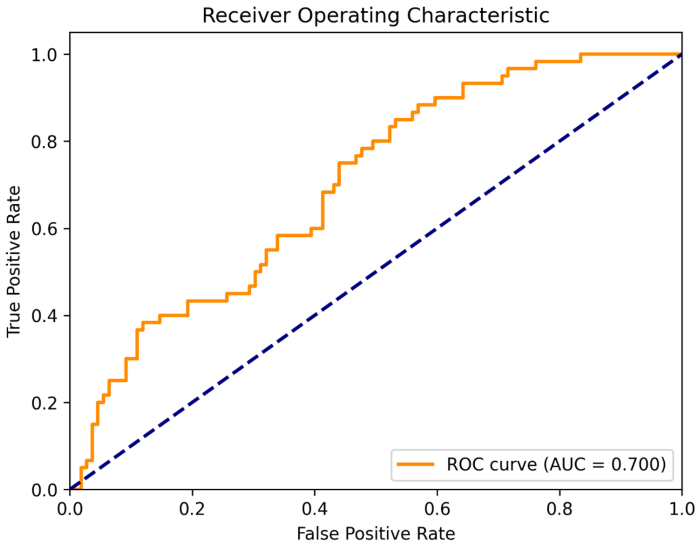

Figure 2. ROC curve analysis model on the predictive value of modeling group moderately severe postoperative pain.

pressure on surrounding tissues, activating pain receptors - an observation consistent across multiple solid tumor types [46-48]. These converging mechanisms underscore the interplay of mechanical, inflammatory, and metabolic factors in post-radiotherapy pain in HBV-related liver cancer.

This study has limitations. The retrospective design limits control over confounding factors such as individual pain thresholds and psychosocial influences, which were not quantitatively assessed. Moreover, the absence of dynamic inflammatory marker monitoring restricted mechanistic exploration at the molecular level. Future research should integrate radiomics, genetic profiling, and longitudinal pain scoring to establish a more comprehensive and precise predictive model.

In conclusion, moderate to severe pain after CyberKnife treatment in HBV-related liver cancer is closely associated with lesion location, baseline liver function, cirrhosis, and tumor size. The nomogram incorporating these factors enables risk stratification and supports individualized analgesic regimens, shifting radiotherapy pain management from uniform protocols toward precision prevention and control. Early identification of high-risk patients and optimized analgesic strategies have the potential to improve treatment outcomes and quality of life.

Disclosure of conflict of interest

None.

Address correspondence to: Jun Jia, Department of Radiotherapy, Senior Department of Oncology, Chinese PLA General Hospital, No. 100 West Fourth Ring Middle Road, Fengtai District, Beijing, China. Tel: +86-010-66933129; E-mail: junjia0930@163.com

References

[1] Iannacone M and Guidotti LG. Immunobiology and pathogenesis of hepatitis B virus infection. Nat Rev Immunol 2022; 22: 19-32.

[2] Adugna A. Histomolecular characterisation of hepatitis B virus induced liver cancer. Rev Med Virol 2023; 33: e2485.

[3] Zoulim F, Chen PJ, Dandri M, Kennedy PT and Seeger C. Hepatitis B virus DNA integration: implications for diagnostics, therapy, and outcome. J Hepatol 2024; 81: 1087-1099.

[4] Yeh SH, Li CL, Lin YY, Ho MC, Wang YC, Tseng ST and Chen PJ. Hepatitis B virus DNA integration drives carcinogenesis and provides a new biomarker for HBV-related HCC. Cell Mol Gastroenterol Hepatol 2023; 15: 921-929.

[5] Yan F, Zhang Q, Shi K, Zhang Y, Zhu B, Bi Y and Wang X. Gut microbiota dysbiosis with hepatitis B virus liver disease and association with immune response. Front Cell Infect Microbiol 2023; 13: 1152987.

[6] Liu Y, Kim ES and Guo H. Hepatitis B virus-related hepatocellular carcinoma exhibits distinct intratumoral microbiota and immune microenvironment signatures. J Med Virol 2024; 96: e29485.

[7] Peneau C, Imbeaud S, La Bella T, Hirsch TZ, Caruso S, Calderaro J, Paradis V, Blanc JF, Letouze E, Nault JC, Amaddeo G and Zucman-Rossi J. Hepatitis B virus integrations promote local and distant oncogenic driver alterations in hepatocellular carcinoma. Gut 2022; 71: 616-626.

[8] Xu Y, Xia C, Li H, Cao M, Yang F, Li Q, Cao M and Chen W. Survey of hepatitis B virus infection for liver cancer screening in China: a population-based, cross-sectional study. Chin Med J (Engl) 2024; 137: 1414-1420.

[9] Ibrahim MK, Liu CD, Zhang L, Yu X, Kim ES, Liu Z, Jo S, Liu Y, Huang Y, Gao SJ and Guo H. The loss of hepatitis B virus receptor NTCP/SLC10A1 in human liver cancer cells is due to epigenetic silencing. J Virol 2024; 98: e0118724.

[10] Nasser N, Tonnerre P, Mansouri A and Asselah T. Hepatitis-B virus: replication cycle, targets, and antiviral approaches. Curr Opin Virol 2023; 63: 101360.
[11] Wongtrakul W, Charoenngam N, Ponvilawan B, Rujirachun P, Wattanachayakul P, Srikulmontri T, Hong N, Rai P and Ungprasert P. Hepatitis B virus infection and risk of gastric cancer: a systematic review and meta-analysis. Minerva Gastroenterol (Torino) 2023; 69: 546-552.
[12] Li Y and Ou JJ. Regulation of mitochondrial metabolism by hepatitis B virus. Viruses 2023; 15: 2359.
[13] Low WF, Ngeow YF, Chook JB, Tee KK, Ong SK, Peh SC, Bong JJ and Mohamed R. Hepatitis B virus DNA methylation and its potential role in chronic hepatitis B. Expert Rev Mol Med 2022; 25: e11.
[14] Min Y, Wei X, Xia X, Wei Z, Li R, Jin J, Liu Z, Hu X and Peng X. Hepatitis B virus infection: an insight into the clinical connection and molecular interaction between hepatitis B virus and host extrahepatic cancer risk. Front Immunol 2023; 14: 1141956.
[15] Lee J, Tsai KN and Ou JJ. Mechanisms of hepatitis B virus-induced hepatocarcinogenesis. Recent Results Cancer Res 2021; 217: 47-70.
[16] Sharma D, Thaper D, Kamal R and Yadav HP. Role of stereotactic body radiotherapy for inferior vena cava tumour thrombus in hepatocellular carcinoma. J Med Imaging Radiat Oncol 2023; 67: 444-449.
[17] Memon B, Kadri S, Sultana N, Saeed K, Ahmed N and Mahmood T. Cyberknife radiosurgery in hepatocellular carcinoma. J Coll Physicians Surg Pak 2021; 31: 532-536.
[18] Que J, Kuo HT, Lin LC, Lin KL, Lin CH, Lin YW and Yang CC. Clinical outcomes and prognostic factors of cyberknife stereotactic body radiation therapy for unresectable hepatocellular carcinoma. BMC Cancer 2016; 16: 451.
[19] Ogino A, Hirai T, Serizawa T and Yoshino A. Clinical features of brain metastases from hepatocellular carcinoma using gamma knife surgery. Acta Neurochir (Wien) 2018; 160: 997-1003.
[20] Zeng Z, Han Y, Li W, Chen H, Lin N, Yu Y and Xu X. Baseline FIB-4 may be a risk factor of recurrence after SBRT in patients with HBV-related small HCC. Cancer Med 2025; 14: e70535.
[21] Zeng M, Tang Z, Ren L, Wang H, Wang X, Zhu W, Mao X, Li Z, Mo X, Chen J, Han J, Kong D, Ji J, Carr AM and Liu C. Hepatitis B virus infection disrupts homologous recombination in hepatocellular carcinoma by stabilizing resection inhibitor ADRM1. J Clin Invest 2023; 133: e171533.
[22] Yoo S, Lee D, Shim JH, Kim KM, Lim YS, Lee HC, Yoo C, Ryoo BY and Choi J. Risk of hepatitis B virus reactivation in patients treated with immunotherapy for anti-cancer treatment. Clin Gastroenterol Hepatol 2022; 20: 898-907.
[23] Arslan F, Franci G, Maria Nastri B and Pagliano P. Hepatitis B virus-induced hepatocarcinogenesis: a virological and oncological perspective. J Viral Hepat 2021; 28: 1104-1109.
[24] Sun R, Li J, Lin X, Yang Y, Liu B, Lan T, Xiao S, Deng A, Yin Z, Xu Y, Xiang Z and Wu B. Peripheral immune characteristics of hepatitis B virus-related hepatocellular carcinoma. Front Immunol 2023; 14: 1079495.
[25] Wu H, Liao B, Li X, Liu H, Gong M, Shi H, Xie S, Guo F, Chen K, Yan R, Zhao H, Li L, Zheng A, Liu Y and Wang Z. Increased hepatitis B virus quasispecies diversity is correlated with liver fibrosis progression. Infect Genet Evol 2021; 93: 104938.
[26] Li Z, Ma L, Di L and Lin X. MicroRNA-1271-5p alleviates the malignant development of hepatitis B virus-mediated liver cancer via binding to AQP5. Mol Med Rep 2021; 23: 386.
[27] Tai J, Harrison AP, Chen HM, Hsu CY, Hsu TH, Chen CJ, Jeng WJ, Chang ML, Lu L and Tai DI. Acoustic radiation force impulse predicts long-term outcomes in a large-scale cohort: high liver cancer, low comorbidity in hepatitis B virus. World J Gastroenterol 2023; 29: 2188-2201.
[28] Kim BH, Lee D, Jung KW, Won YJ and Cho H. Cause of death and cause-specific mortality for primary liver cancer in South Korea: a nationwide population-based study in hepatitis B virus-endemic area. Clin Mol Hepatol 2022; 28: 242-253.
[29] Pujol F, Jaspe RC, Loureiro CL and Chemin I. Hepatitis B virus American genotypes: pathogenic variants? Clin Res Hepatol Gastroenterol 2020; 44: 825-835.
[30] Zhang Y, Cao W, Wang S, Zhang L, Li X, Zhang Z, Xie Y and Li M. Epigenetic modification of hepatitis B virus infection and related hepatocellular carcinoma. Virulence 2024; 15: 2421231.
[31] de Mattos AZ, Debes JD, Boonstra A, Yang JD, Balderramo DC, Sartori GDP and de Mattos AA. Current impact of viral hepatitis on liver cancer development: the challenge remains. World J Gastroenterol 2021; 27: 3556-3567.
[32] Lee JH. Old hepatitis B virus never dies: it just hides itself within the host genome. Clin Mol Hepatol 2021; 27: 107-109.
[33] Qiu S, Jin L, Yang D and Zhang D. Clinical application value of hepatitis B virus basal core promoter 1762/1764 and GGTII and GGT in patients with HBV-DNA-positive primary liver cancer. Medicine (Baltimore) 2023; 102: e35699.

[34] Gu S, Lv L, Lin X, Li X, Dai J, Zhang J, Kong R, Xie W and Li J. Using structural analysis to explore the role of hepatitis B virus mutations in immune escape from liver cancer in Chinese, European and American populations. J Biomol Struct Dyn 2022; 40: 1586-1596.
[35] Yu C, Li J, Li Q, Chang S, Cao Y, Jiang H, Xie L, Fan G and Wang S. Hepatitis B virus (HBV) codon adapts well to the gene expression profile of liver cancer: an evolutionary explanation for HBV's oncogenic role. J Microbiol 2022; 60: 1106-1112.
[36] Tu T, Zhang H and Urban S. Hepatitis B virus DNA integration: in vitro models for investigating viral pathogenesis and persistence. Viruses 2021; 13: 180.
[37] Schollmeier A, Glitscher M and Hildt E. Relevance of HBx for hepatitis B virus-associated pathogenesis. Int J Mol Sci 2023; 24: 4964.
[38] Zhang Y, Zhao S, Ding H, Song X, Miao H, Cui X, Wang J and Han B. Big data information under proportional hazard mathematical model in analysis of hepatitis B virus infection data of patients with interventional liver cancer through antiviral therapy of entecavir. J Healthc Eng 2021; 2021: 6225403.
[39] Yu S, Gao W, Zeng P, Chen C, Liu Z, Zhang Z and Liu J. Exploring the effect of polyphyllin I on hepatitis B virus-related liver cancer through network pharmacology and in vitro experiments. Comb Chem High Throughput Screen 2022; 25: 934-944.
[40] Rim CH, Park S, Yoon WS, Shin IS and Park HC. Radiotherapy for bone metastases of hepatocellular carcinoma: a hybrid systematic review with meta-analyses. Int J Radiat Biol 2023; 99: 419-430.
[41] Kim TH, Koh YH, Kim BH, Kim MJ, Lee JH, Park B and Park JW. Proton beam radiotherapy vs. radiofrequency ablation for recurrent hepatocellular carcinoma: a randomized phase III trial. J Hepatol 2021; 74: 603-612.
[42] Dawson LA, Ringash J, Fairchild A, Stos P, Dennis K, Mahmud A, Stuckless TL, Vincent F, Roberge D, Follwell M, Wong RKW, Jonker DJ, Knox JJ, Zimmermann C, Wong P, Barry AS, Gaudet M, Wong RKS, Purdie TG, Tu D and O'Callaghan CJ. Palliative radiotherapy versus best supportive care in patients with painful hepatic cancer (CCTG HE1): a multicentre, open-label, randomised, controlled, phase 3 study. Lancet Oncol 2024; 25: 1337-1346.
[43] Luo Y, Huang X, Chen J and Zhang S. Evaluation of the clinical efficacy of intensity-modulated radiotherapy combined with transcatheter arterial chemoembolization for hepatocellular carcinoma with extrahepatic oligometastasis and prognostic factors for patient survival. Int J Gen Med 2023; 16: 1271-1278.
[44] Kim K, Lee J and Seong J. Skull base metastasis from hepatocellular carcinoma: clinical presentation and efficacy of radiotherapy. J Hepatocell Carcinoma 2022; 9: 357-366.
[45] Gong Y, Zeng F, Zhang F, Liu X, Li Z, Chen W, Liu H, Li X, Cheng Y, Zhang J, Feng Y, Wu T, Zhou W and Zhang T. Radiotherapy plus a self-gelation powder encapsulating tRF5-GlyGCC inhibitor potentiates natural kill cell immunity to prevent hepatocellular carcinoma recurrence. J Nanobiotechnology 2025; 23: 100.
[46] Sarwar A, Malik MS, Vo NH, Tsai LL, Tahir MM, Curry MP, Catana AM, Bullock AJ, Parker JA, Eckhoff DE, Nasser IA, Weinstein JL and Ahmed M. Efficacy and safety of radiation segmentectomy with (90)Y resin microspheres for hepatocellular carcinoma. Radiology 2024; 311: e231386.
[47] Ferini G, Palmisciano P, Scalia G, Haider AS, Bin-Alamer O, Sagoo NS, Bozkurt I, Deora H, Priola SM, Aoun SG and Umana GE. The role of radiation therapy in the treatment of spine metastases from hepatocellular carcinoma: a systematic review and meta-analysis. Neurosurg Focus 2022; 53: E12.
[48] Chen CY, Huang BS, Hong JH, Chang JT, Chen MC, Tang WR, Shun SC and Chen ML. Persistent fatigue in patients with hepatocellular carcinoma receiving radiotherapy. J Nurs Res 2024; 32: e319.